Incorporation of metabolically stable ketones into a small molecule probe to increase potency and water solubility

Marie-Helene Larraufie [a], Wan Seok Yang [a], Elise Jiang [b], Ajit G. Thomas [c], Barbara S. Slusher [c,d], Brent R. Stockwell [a,b,e,*]

[a] Department of Biological Sciences, Columbia University, 550 West 120th Street, 1208 Northwest Corner Building, MC 4846, New York, NY 10027, United States
[b] Department of Chemistry, Columbia University, New York, NY 10027, United States
[c] Brain Science Institute, Johns Hopkins Medicine, Baltimore, United States
[d] Department of Neurology, Johns Hopkins Medicine, Baltimore, United States
[e] Howard Hughes Medical Institute, Columbia University, New York, NY 10027, United States

ARTICLE INFO

ABSTRACT

Introducing a reactive carbonyl to a scaffold that does not otherwise have an electrophilic functionality to create a reversible covalent inhibitor is a potentially useful strategy for enhancing compound potency. However, aldehydes are metabolically unstable, which precludes the use of this strategy for compounds to be tested in animal models or in human clinical studies. To overcome this limitation, we designed ketone-based functionalities capable of forming reversible covalent adducts, while displaying high metabolic stability, and imparting improved water solubility to their pendant scaffold. We tested this strategy on the ferroptosis inducer and experimental therapeutic erastin, and observed substantial increases in compound potency. In particular, a new carbonyl erastin analog, termed IKE, displayed improved potency, solubility and metabolic stability, thus representing an ideal candidate for future in vivo cancer therapeutic applications.

© 2015 Published by Elsevier Ltd.

There is growing awareness that compounds with optimal properties in terms of selectivity and potency might be obtained by combining the distinct properties of covalent and non-covalent ligands.[1] Practically, this often means functionalizing a scaffold optimized for specific complementarity to a target with a carefully tuned reactive moiety, to create a targeted covalent inhibitor. A powerful way to mitigate the risks of off-target reactivity is to use a reactive moiety that forms a reversible covalent bond with proteins. In addition to increased selectivity, reversible covalent inhibitors may limit the risk of haptenization and immunogenicity associated with the formation of circulating irreversibly modified protein adducts.[2–5]

An important class of reversible covalent inhibitors are aldehyde-based compounds capable of forming an imine with a lysine side chain in the binding site of a target protein. Recent examples include the IRE1 endonuclease inhibitors 4μ8c[6] and STF083010,[7] a 20S proteasome inhibitor[8] and the tau fibrillization inhibitor oleocanthal.[9] While such reversible covalent inhibitors have mostly been discovered serendipitously, the rational design of selective imine-forming electrophiles may be feasible via the identification of accessible lysine residues and simulation-based pK_a calculations.[10] Indeed, it appears from recent literature that lysines buried in hydrophobic pockets, such as those targeted by small-molecules, have their pK_a downshifted by 3–5 units compared to solvent-exposed lysines.[11,12] This feature would favor the deprotonation of buried lysine side chains and increased nucleophilicity, facilitating selective attack on a proximal carbonyl functionality.

Introducing an aldehyde moiety to an otherwise non-covalent ligand to convert it into a reversible covalent inhibitor may thus be feasible. However, the low metabolic stability of aldehydes generally precludes their utilization for in vivo applications. Indeed, mammals have evolved a range of enzymes to transform aldehydes into the corresponding alcohols (aldoketo reductases) and carboxylic acids (aldehyde dehydrogenases/cytochromes P450s).[13] No carbonyl moieties capable of forming imines with lysine side chains have been described that are also metabolically stable. Described herein is the design and synthesis of such functionalities, with optimized metabolic stability and aqueous solubility, and their incorporation into the scaffold of the small molecule ferroptosis probe erastin.

We previously showed that erastin induces preferential lethality in engineered human fibroblasts overexpressing oncogenic HRAS.[14]

* Corresponding author.
  E-mail address: bstockwell@columbia.edu (B.R. Stockwell).

ARTICLE IN PRESS

2   M.-H. Larraufie et al./Bioorg. Med. Chem. Lett. xxx (2015) xxx–xxx

Erastin induces an oxidative form of non-apoptotic cell death, termed ferroptosis,[15] that is regulated by glutathione peroxidase 4.[16] Erastin (Fig. 1, ERA) exhibits modest water solubility (0.086 mM) and potency (GI$_{50}$ = 1.7 μM in HRAS^{G12V}-overexpressing tumorigenic cells BJeLR), precluding its use in vivo. Introducing a piperazine moiety on the *meta* position of the aniline ring of erastin enhances the water solubility of the scaffold. This piperazine erastin analog (Fig. 1, PE) displayed significant activity in a tumor prevention model using nude mice injected with *NRAS* mutant human HT-1080 fibrosarcoma cells, in which PE was injected before tumors became established.[16] However, PE had a limited effect on the growth of already established tumors, perhaps due to its moderate potency. Replacing the piperazine moiety with an aldehyde functionality (Fig. 1, AE) allowed a substantial increase in potency, albeit at the expense of metabolic stability and solubility.[16] Nevertheless, this large increase in potency brought about by the introduction of an aldehyde moiety suggested that a lysine side chain in the vicinity of the binding site was susceptible to imine formation. We consequently endeavored to design carbonyl-containing analogs with an optimal balance between reactivity, stability and solubility, and tested the consequences of their incorporation into the erastin scaffold. Using this strategy, we identified erastin analogs with metabolically stable electrophilic ketones, and improved potency and metabolic stability compared to erastin and PE.

α-Substituted ketones can form imines with lysine side chain. In order to define the structural requirements for facile imine formation, we compared the reactivity of aryl aldehydes and α-substituted aryl ketones towards a simple model of lysine side chain. Our idea was to use *n*-butyl amine to mimic the reactive side chain of lysine and determine whether this moiety could react with α-substituted ketones at 37 °C. Reaction of aryl aldehyde **1a** with *n*-butylamine in MeOH produced imine **2a** with >90% conversion after 24 h at 37 °C. High conversion to the imine adduct were also obtained with methyl ketone **1b** and α-fluoromethyl ketone **1c**. We observed that when the methyl ketone was α-substituted with heterocycles, the formation of the imine adduct could still be observed, although the conversion was lower under these conditions. We tested in total a set of 9 carbonyl-containing moieties after 24 h at 37 °C (Fig. 2). We found that α-substituted ketones could be used as an electrophile for imine formation, and the relative reactivity of each carbonyl moiety was determined.

Synthesis of carbonyl erastin analogs: We endeavored to develop an efficient synthetic strategy to incorporate reactive carbonyl moieties in the *meta* position of the aniline-derived moiety of erastin, as a model for incorporating such functionalities on aromatic regions of small molecules generally. A methyl ketone derivative, KE (Fig. 3, entry 4), was synthesized in 5 steps (overall yield 21%) from commercially available 4-hydroxy-3-nitroacetophenone (see Supporting information). Similarly, α-fluoro ketone erastin (FKE) and trifluoroketone erastin (TFKE) (Fig. 3, entries 5 and 6) were prepared in 6 steps from 4-hydroxy-3-nitroacetophenone and 3-nitrophenol, respectively, (see Supporting information). Finally, we synthesized morpholine ketone erastin (MKE), *N*-methylpiperazine ketone erastin (MPKE), *N*-allylpiperazine ketone erastin (APKE), *N-p*-methoxybenzylpiperazine ketone erastin (PMB-PKE), piperazine ketone erastin (PKE) and imidazole ketone erastin (IKE) (Fig. 3, entries 7–12) using the general synthetic route depicted in Scheme 1 for APKE and PKE.

Carbonyl erastin analogs are potent system x$_c^-$ inhibitors: We previously demonstrated that erastin induces ferroptosis via the inhibition of cystine uptake through the cystine–glutamate
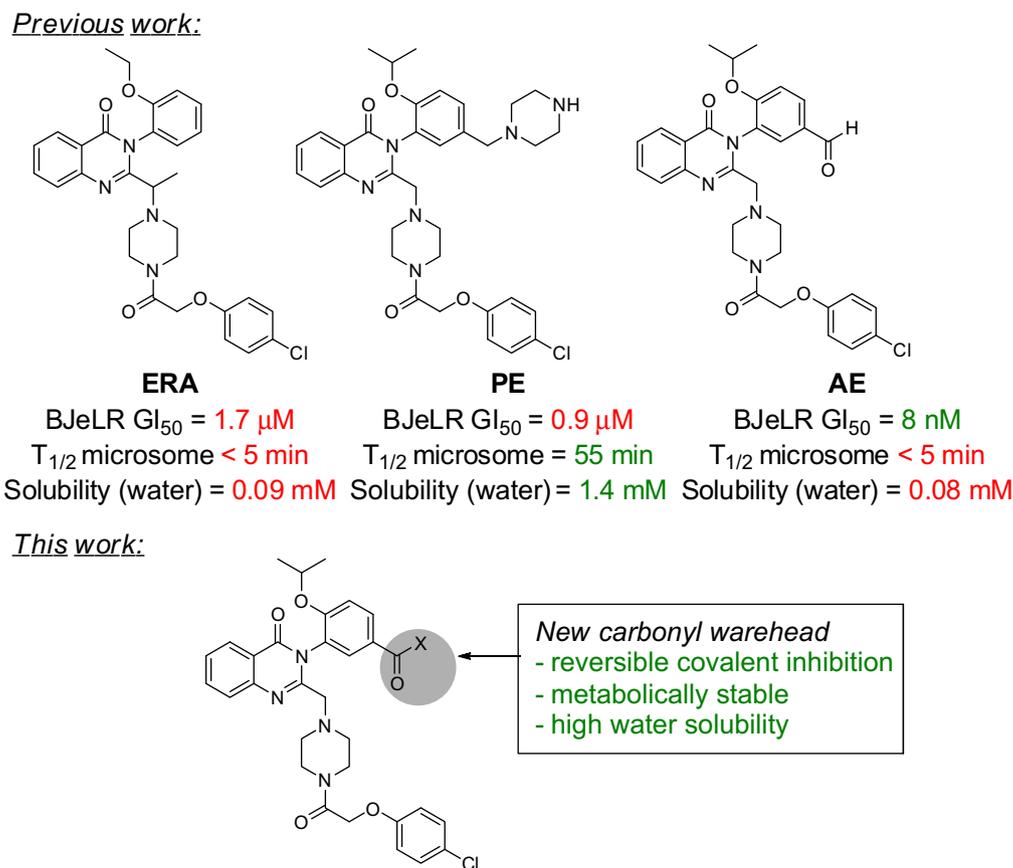
Previous work:

ERA
BJeLR GI$_{50}$ = 1.7 μM
T$_{1/2}$ microsome < 5 min
Solubility (water) = 0.09 mM

PE
BJeLR GI$_{50}$ = 0.9 μM
T$_{1/2}$ microsome = 55 min
Solubility (water) = 1.4 mM

AE
BJeLR GI$_{50}$ = 8 nM
T$_{1/2}$ microsome < 5 min
Solubility (water) = 0.08 mM

This work:

New carbonyl warehead
- reversible covalent inhibition
- metabolically stable
- high water solubility

Figure 1. Structure of erastin analogs (top) and design of analogs (bottom) with improved properties.

ARTICLE IN PRESS

M.-H. Larraufie et al./Bioorg. Med. Chem. Lett. xxx (2015) xxx–xxx

3

| Probe, X	Imine/SM ratio	Probe, X	Imine/SM ratio
1a, X = H	10/1	**1b**, X = Me	3/1
1c, X = CH$_2$F	1/1		
1d, X =	1/1.2	**1e**, X =	1/2.5
1f, X =	1/1.2	**1g**, X =	1/4
1h, X =	1/7	**1i**, X =	1/1.5
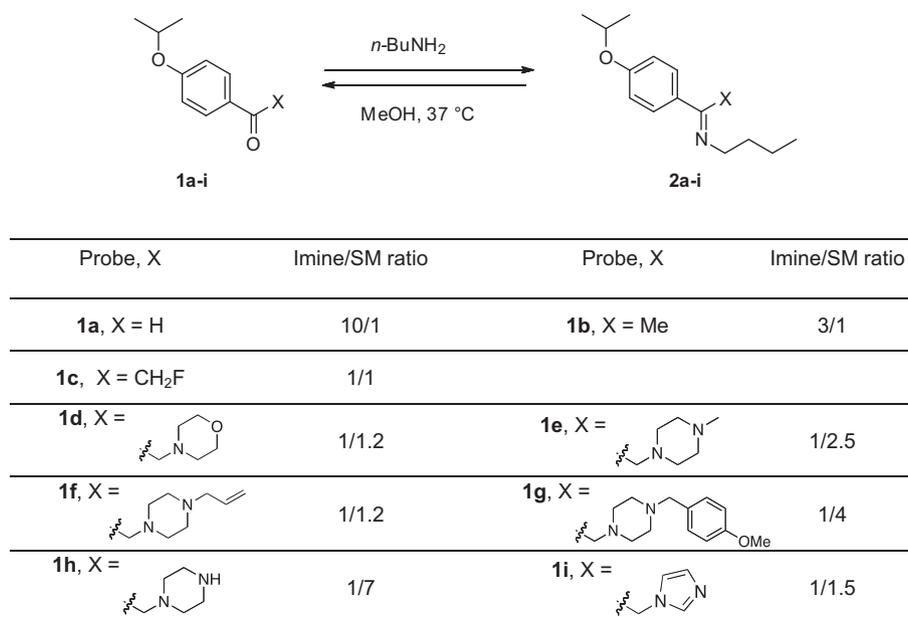
Figure 2. Comparative reactivities of carbonyl moieties with *n*-butylamine. Carbonyl derivative **1a–i** were reacted with *n*-butylamine in MeOH, and the imine adduct to starting material ratio (imine/SM) was measured after 24 h by treating the mixture with NaBH$_3$CN, and isolating the corresponding amine and SM.
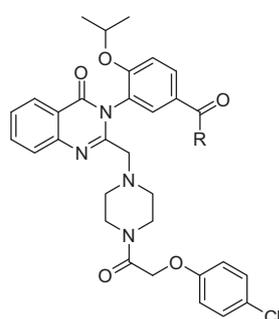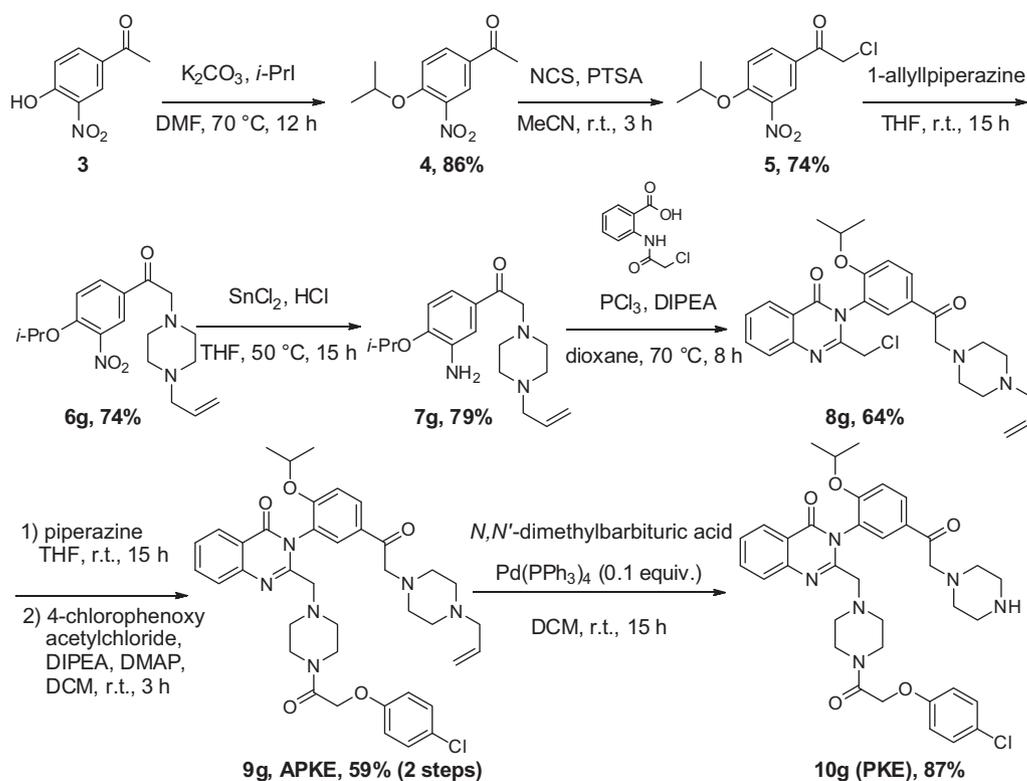

Entry	Compound	R	IC$_{50}$ glutamate release (nM)
1	Erastin	See fig.1	200
2	PE	See fig. 1	800
3	AE	H	60
4	KE	Me	30
5	FKE	CH$_2$F	40
6	TFKE	CF$_3$	20
7	MKE		10
8	MPKE		300
9	APKE		10
10	PMB-PKE		4
11	PKE		100
12	IKE		30

Figure 3. Erastin analogs potencies in glutamate-release assay.

antiporter (system x$_c^-$).[15] The ten ketone erastin analogs were evaluated in a glutamate release assay, which reports on system x$_c^-$ activity. Human astrocytoma cells (CCF-STTG1) were used, which contain the system x$_c^-$.[17] Following a 2 h incubation period, glutamate released into the medium was detected fluorometrically using glutamate oxidase, horseradish peroxidase and Amplex UltraRed. Dramatic improvement of the half-maximal inhibitory constants (IC$_{50}$) for system x$_c^-$ inhibition was observed for all ketone analogs, compared to erastin and PE (Fig. 3). Several analogs, such as MKE (Fig. 3, entry 7, IC$_{50}$ = 10 nM) and IKE (Fig. 3, entry 12, IC$_{50}$ = 30 nM) even had improved potency over aldehyde erastin (Fig. 3, entry 3, IC$_{50}$ = 60 nM).

Carbonyl erastin analogs exhibit selective lethality in BJ-derived tumorigenic cells expressing oncogenic HRAS: Encouraged by this improved potency in the system x$_c^-$ assay, we tested the potency and genotype-selective lethality of the ketone analogs in BJ-derived cell lines. Compounds were tested in 4 isogenic cell lines: HRAS^{G12V}-overexpressing tumorigenic cells (BJeLR, DRD) and non-transformed isogenic cells without mutant HRAS expression (BJeHLT, BJeH). We observed that all the analogs except MPKE and APKE were preferentially lethal to BJeLR and DRD cells compared to BJeH and BJeHLT cells (Figs. 4A and S1). In addition, AE, KE, FKE, PKE and IKE demonstrated low nanomolar potencies in the HRAS^{G12V}-overexpressing cell lines.

ARTICLE IN PRESS

4   M.-H. Larraufie et al./Bioorg. Med. Chem. Lett. xxx (2015) xxx–xxx

Scheme 1. Synthetic route to piperazine ketone erastin (PKE).

B

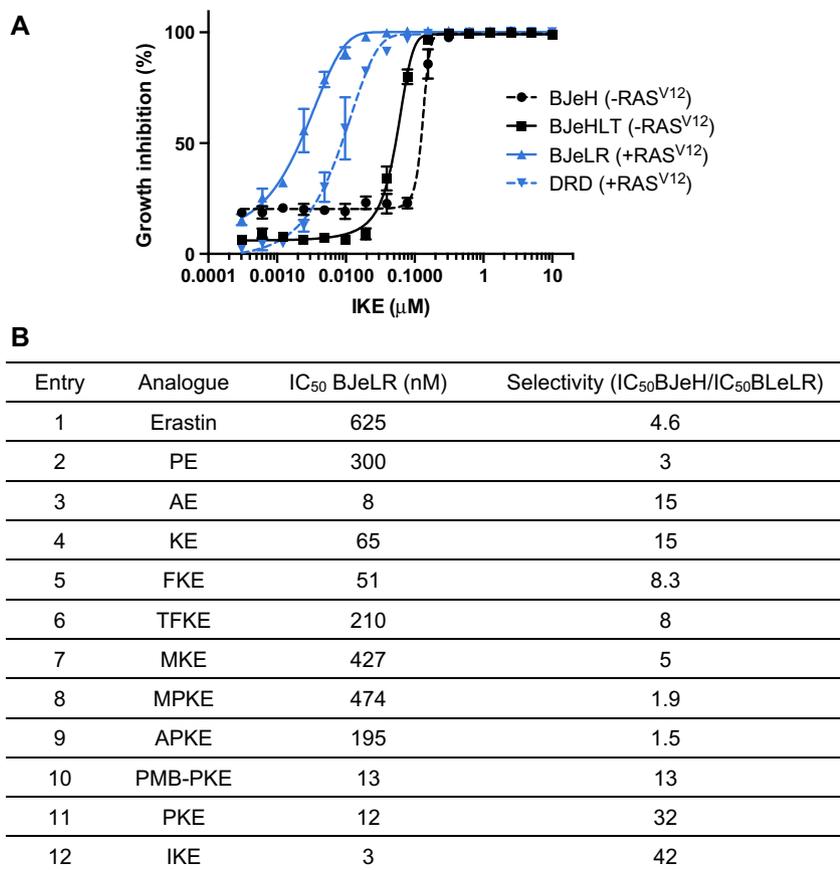| Entry	Analogue	IC$_{50}$ BJeLR (nM)	Selectivity (IC$_{50}$BJeH/IC$_{50}$BLeLR)
1	Erastin	625	4.6
2	PE	300	3
3	AE	8	15
4	KE	65	15
5	FKE	51	8.3
6	TFKE	210	8
7	MKE	427	5
8	MPKE	474	1.9
9	APKE	195	1.5
10	PMB-PKE	13	13
11	PKE	12	32
12	IKE	3	42

Figure 4. Selective lethality of carbonyl erastin analogs in BJ-derived cell lines. (A) Growth inhibition of BJ cell lines after 24 h treatment with IKE. (B) Erastin analog potencies and selectivities in BJ cells.

ARTICLE IN PRESS

M.-H. Larraufie et al. / Bioorg. Med. Chem. Lett. xxx (2015) xxx–xxx 5

In addition, we evaluated the ability of IKE and PKE to inhibit the growth of highly tumorigenic HT-1080 human fibrosarcoma cell line. Treatment of HT-1080 cells for 48 h with either PKE or IKE resulted in complete growth inhibition. We determined that IKE (GI_{50} = 310 nM) was almost twice as potent as PKE (GI_{50} = 550 nM) in this cell line (see Fig. S2).

Two carbonyl erastin analogs, IKE and PKE display high metabolic stability: Our rationale for the design of new carbonyl warheads was that the substitution of the methylene alpha to the ketone carbonyl with polar bulky moieties would both enhance the water solubility of the analogs and hamper metabolic degradation (e.g., reduction) of that sensitive position by cytochrome P450 enzymes. We assessed experimentally the half-lives of the eight most potent analogs in mouse liver microsomes. The carbonyl erastin analogs were incubated at 37 °C for up to 45 minutes in potassium phosphate buffer (pH 7.4) containing mouse liver microsomal proteins and an NADPH-generating system. At 0, 5, 15, 30 and 45 min intervals, aliquots were removed and analyzed by LC–MS/MS to determine the half-life and the intrinsic clearance of each compound (see Fig. S3). As predicted, both the aldehyde analog (Fig. 5, AE) and the methyl ketone analog (Fig. 5, KE) were rapidly metabolized and had half-lives <5 min. Several other carbonyl erastin analogs (Fig. 5: FKE, MPKE, APKE, PMB-PKE) displayed medium to poor metabolic stability. On the other hand, to our delight, two carbonyl erastin analogs, piperazine ketone erastin (Fig. 5, PKE, $T_{1/2}$ >90 min) and imidazole ketone erastin (Fig. 5, IKE, $T_{1/2}$ = 79 min) demonstrated exceptionally high metabolic stability that even surpassed that of piperazine erastin, which does not possess a carbonyl functionality (Fig. 5, PKE, $T_{1/2}$ = 55 min).

In addition, we assessed the plasma stability and PK profile of IKE and PKE in mice. Stability of PKE and IKE in mouse plasma was determined by dissolving each compound in the mouse plasma at 500 ng/mL concentration followed by incubation at 37 °C. Both PKE and IKE remained stable up until 120 min under this condition.

The design of covalent inhibitors has recently attracted renewed interest, with several covalent drug candidates now progressing to late-stage clinical trials.[1] This renaissance stems in part from the greater appreciation that low doses of highly potent targeted covalent inhibitors have few off-target effects,[18,19] and that reversible covalent inhibitors are even less likely to exhibit immunotoxicity.[20]

Although most current covalent drugs were discovered through serendipity, there is now an interest in the explicit design of targeted covalent inhibitors. The design of such compounds involves identifying a non-covalent scaffold with high potency, followed by functionalization with moieties capable of forming covalent

interactions.[21–25] Here, we reported the design of ketone moieties able to engage in reversible imine formation with lysine residues. In contrast to an aldehyde, these optimized ketone moieties are metabolically stable and can enhance the solubility of the pendant scaffold. They are thus promising functionalities to append to otherwise non-covalent inhibitors in order to improve potency and solubility without compromising metabolic stability. We demonstrated the validity of this approach by functionalizing the small molecule probe erastin with carbonyl warheads. The carbonyl erastin analogs demonstrated clear increased potency as system x_c^- inhibitors, compared to erastin and piperazine erastin. In addition, two ketone erastin analogs, PKE and IKE, displayed low nanomolar potency and selective lethality towards BJ-derived tumorigenic cells expressing oncogenic *HRAS*. Use of these ketone moieties has resulted in the creation of a ketone erastin analog, IKE, with optimized properties for in vivo use, which represents a decisive milestone in the development of therapeutic ferroptosis inducers. In addition, this successful application highlights the potential of these rationally designed carbonyl warhead for improving compounds for in vivo applications.

Supplementary data

Supplementary data associated with this article can be found, in the online version, at http://dx.doi.org/10.1016/j.bmcl.2015.07.018.

References and notes

1. Singh, J.; Petter, R. C.; Baillie, T. A.; Whitty, A. *Nat. Rev. Drug Disc.* **2011**, *10*, 307.
2. Serafimova, I. M.; Pufall, M. A.; Krishnan, S.; Duda, K.; Cohen, M. S.; Maglathlin, R. L.; Mcfarland, J. M.; Miller, R. M.; Frödin, M.; Taunton, J. *Nat. Chem. Biol.* **2012**, *8*, 471.
3. Miller, R. M.; Paavilainen, V. O.; Krishnan, S.; Serafimova, I. M.; Taunton, J. *J. Am. Chem. Soc.* **2013**, *135*, 5298.
4. Lee, C.-U.; Grossmann, T. N. *Angew. Chem., Int. Ed.* **2012**, *51*, 8699.
5. Patch, R. J.; Searle, L. L.; Kim, A. J.; De, D. Y. D.; Zhu, X. Z.; Askari, H. B.; ONeill, J. C.; Abad, M. C.; Rentzeperis, D.; Liu, J. Y.; Kemmerer, M.; Lin, L.; Kasturi, J.; Geisler, J. G.; Lenhard, J. M.; Player, M. R.; Gaul, M. D. *J. Med. Chem.* **2011**, *54*, 788.
6. Cross, B. C. S.; Bond, P. J.; Sadowski, P. G.; Jha, B. K.; Zak, J.; Goodman, J. M.; Silverman, R. H.; Neubert, T. A.; Baxendale, I. R.; Ron, D.; Harding, H. P. *Proc. Natl. Acad. Sci. U.S.A.* **2012**, *109*, E869.
7. Papandreou, I.; Denko, N. C.; Olson, M.; Van Melckebeke, H.; Lust, S.; Tam, A.; Solow-Cordero, D. E.; Bouley, D. M.; Offner, F.; Niwa, M.; Koong, A. C. *Blood* **2011**, *117*, 1311.
8. Ma, Y.; Xu, B.; Fang, Y.; Yang, Z.; Cui, J.; Zhang, L.; Zhang, L. *Molecules* **2011**, *16*, 7551.
9. Li, W.; Sperry, J. B.; Crowe, A.; Trojanowski, J. Q.; Smith, A. B., III; Lee, V. M.-Y. *J. Neurochem.* **2009**, *110*, 1339.
10. Tomasio, S. M.; Harding, H. P.; Ron, D.; Cross, B. C. S.; Bond, P. J. *Mol. BioSyst.* **2013**, *9*, 2408.
11. Barbas, C. F., III; Heine, A.; Zhong, G.; Hoffmann, T.; Gramatikova, S.; Bjornestedt, R.; List, B.; Anderson, J.; Stura, E. A.; Wilson, I. A.; Lerner, R. A. *Science* **1997**, *278*, 2085.
12. Isom, D. G.; Castañeda, C. A.; Cannon, B. R.; Garcia-Moreno, E. B. *Proc. Natl. Acad. Sci. U.S.A.* **2011**, *108*, 5260.
13. Conklin, D.; Prough, R.; Bhatanagar, A. *Mol. BioSyst.* **2007**, *3*, 136.
14. Dolma, S.; Lessnick, S. L.; Hahn, W. C.; Stockwell, B. R. *Cancer Cell* **2003**, *3*, 285.
15. Dixon, S. J.; Lemberg, K. M.; Lamprecht, M. R.; Skouta, R.; Zaitsev, E. M.; Gleason, C. E.; Patel, D. N.; Bauer, A. J.; Cantley, A. M.; Yang, W. S.; Morrison, B.; Stockwell, B. R. *Cell* **2012**, *149*, 1060.
16. Yang, W. S.; SriRamaratnam, R.; Welsch, M. E.; Shimada, K.; Skouta, R.; Viswanathan, V. S.; Cheah, J. H.; Clemons, P. A.; Shamji, A. F.; Clish, C. B.; Brown,
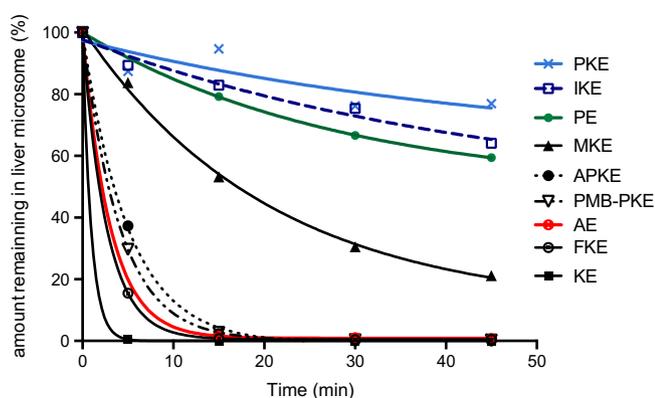
Figure 5. Metabolic stability of carbonyl erastin analogs in mouse liver microsomes.

M.-H. Larraufie et al. / Bioorg. Med. Chem. Lett. xxx (2015) xxx–xxx

L. M.; Girotti, A. W.; Cornish, V. W.; Schreiber, S. L.; Stockwell, B. R. *Cell* **2014**, *156*, 317.

17. Dixon, S. J.; Patel, D. N.; Welsch, M. E.; Skouta, R.; Lee, E. D.; Hayano, M.; Thomas, A. G.; Gleason, C. E.; Tatonetti, N. P.; Slusher, B. S.; Stockwell, B. R. *eLife* **2014**, *3*, e02523.

18. Wu, H.; Wang, W.; Liu, F.; Weisberg, E. L.; Tian, B.; Chen, Y.; Li, B.; Wang, A.; Wang, B.; Zhao, Z.; McMillin, D. W.; Hu, C.; Li, H.; Wang, J.; Liang, Y.; Buhrlage, S. J.; Liang, J.; Liu, J.; Yang, G.; Brown, J. R.; Treon, S. P.; Mitsiades, C. S.; Griffin, J. D.; Liu, Q.; Gray, N. S. *ACS Chem. Biol.* **2014**, *9*, 1086.

19. Lanning, B. R.; Whitby, L. R.; Dix, M. M.; Douhan, J.; Gilbert, A. M.; Hett, E. C.; Johnson, T. O.; Joslyn, C.; Kath, J. C.; Niessen, S.; Roberts, L. R.; Schnute, M. E.;

Wang, C.; Hulce, J. J.; Wei, B.; Whiteley, L. O.; Hayward, M. M.; Cravatt, B. F. *Nat. Chem. Biol.* **2014**, *10*, 760.

20. Maha, R.; Thomas, J. R.; Shafer, C. M. *Bioorg. Med. Chem. Lett.* **2014**, *24*, 33.

21. Cohen, M. S.; Zhang, C.; Shokat, K. M.; Taunton, J. *Science* **2005**, *308*, 1318.

22. Zhou, W.; Hur, W.; McDermott, U.; Dutt, A.; Xian, W.; Ficarro, S. B.; Zhang, J.; Sharma, S. V.; Brugge, J.; Meyerson, M., et al. *Chem. Biol.* **2010**, *17*, 285.

23. Kwarcinski, F. E.; Fox, C. C.; Steffey, M. E.; Soellner, M. B. *ACS Chem. Biol.* **2012**, *7*, 1910.

24. Ward, R. A. et al *J. Med. Chem.* **2013**, *56*, 7025.

25. Zhang, T. et al *Chem. Biol.* **2012**, *19*, 140.